

¹Prasad SANATAN, ²Prasad ANANT, ³Kumar ARBIND

MATERIAL ONTO A LOW MELTING TEMPERATURE CYLINDRICAL SOLID ADDITIVE OF NEGLIGIBLE THERMAL RESISTANCE

¹R.V.S. College of Engineering and Technology, Jamshedpur, INDIA

²National Institute of Technology, Jamshedpur, INDIA

³Birla Institute of Technology, Mesra, Ranchi, INDIA

Abstract: Current investigation devises a non-dimensional lump-integral model for reduction in time of occurrence of unavoidable freezing and melting of the bath material onto a low melting temperature cylindrical solid additive of negligible thermal resistance during the melt preparation of required composition for production of steel. Such a reduction decreases the production time, cost, energy requirement and environmental impact and increases the productivity for global competitiveness. This model regulates such an event by the bath condition denoted by modified conduction factor, C_{ofm} , the melt temperature-ratio, θ_{ab} , and the heat-capacity ratio, C_r , the phase-change parameters: Stefan number, S_{ta} of the additive, and that of the bath material, S_{tb} and gives solutions in terms of these parameters. During this event, the additive undergoes pre-melt heating, melting at its melting temperature and post-melt heating up to freezing temperature of bath material stages. The first and third stages solutions are numeric whereas the second stage solution is in closed-form. The total time of freezing and melting reduces when C_{ofm} decreases or either S_{tb} or C_r increases whereas this time insignificantly diminishes by change in either S_{ta} or θ_{ab} . For each of these parameters other parameters are prescribed. The first stage is validated with that of the literature by converting its model to heating the additive without freezing the bath material onto it.

Keywords: alloyants addition, alloyants-melt bath system, mathematical modelling, freezing and melting

1. INTRODUCTION

Due to stiff competition and glut in the global market, steel-makers are required to manufacture steel and cast iron of different constituents at low cost, with high productivity and without degrading their quality. To produce them, their melt is first prepared by dunking and assimilating the additive in the hot metal bath and then passed through several metallurgical processes before it is cast. Here, an undesirable freezing and melting of the bath material onto the additive not required in the preparation of the melt occurs as soon as it is dunked in the bath.

The occurrence is due to the development of large temperature gradient towards the additive side compared with that of the bath side immediately after the additive is dunked in the bath. It leads to the requirement of heat to be conducted to the additive much larger than the convective heat available from the bath for thermal equilibrium. The excess of this conductive heat is compensated by the latent heat of fusion generated from the freezing of the bath material onto the additive. As the time elapses, this heat conducted increases the additive temperature, reduces the temperature gradient at the additive side and the rate of the development of the frozen layer. Ultimately, the heat conducted to the additive decreases so much that the convective heat of the bath becomes larger resulting in melting of the frozen layer completely by the excess of the convective heat exposing the original additive at a raised temperature.

This unavoidable event takes certain time and increases the production time of their manufacturing. In view of this, the temperature gradient, which is regulated by the order of magnitude of the ratio of the thermal resistance of the additive and that of the convective heat of bath including the frozen layer, acts as a controlling parameter for the time of the freezing and melting and consequently, the production time, such a ratio is recognised as Biot number, B_i . When B_i is reduced to lower than 0.1 ($B_i < 1$), it diminishes the temperature gradient towards the additive side so much that the temperature distribution becomes uniform in the additive and the conductive heat requirement gets reduced appreciably. It, in turn, increases the difference of bath convective heat and conductive heat allowing the formation of smaller thickness of the frozen layer onto the additive. It takes less time to melt. Thus, the completion time of freezing and melting reduces decreasing the production time.

The literature does not contain the investigation of this situation for the freezing and melting of the bath material onto a low melting temperature cylindrical additive. Nevertheless, when the thermal resistance of the additive is comparable with that of the bath, the freezing and melting of the bath material onto the spherical [1-6], cylindrical [7-10] and plate [11] shaped additives were studied. It was also analysed for the plate and cylindrical additives [12,13] when the thermal resistance of the frozen layer developed onto them was

negligible with respect to that of the additive and for the cylindrical additive having negligible thermal resistance [14,15] as compared with the thermal resistance of the bath including the frozen layer. The melting temperature of these additives was assumed to be higher than the freezing temperature of the bath material. It was predicted that diminishing the radius of spherical additive made of aluminium in the salt melt bath [16], slag in slag melt bath [1] and ferro-manganese in the steel bath [6] reduces the time of freezing and melting of the bath material. This time was also estimated for the frozen layer developed of negligible thermal resistance with respect to that of the additive in case of sponge iron [17] and ferro-manganese [18] spherical additives. For the cylindrical additive of steel [7], titanium [8,9], niobium [19] and zirconium [20], the freezing and melting time of the bath material around them was found to decrease once their radius was reduced. The instance interface temperature between the cylindrical additive having high [21] or low [22] melting temperature than that of the bath material and the freezing layer of the bath material onto it soon after immersing it in the bath was obtained in closed-form. For the high melting temperature plate additive [23], this temperature was also found as a closed-form expression.

In the current work, axi-symmetric freezing and melting of a bath material onto a low melting temperature cylindrical additive is investigated, in case, the additive thermal resistance is negligible with respect to that of the bath including the frozen layer. Its mathematical model in a non-dimensional lump-integral format is designed indicating this event dependence on the non-dimensional independent parameters; the melting temperature - ratio, θ_{ab} , the heat capacity-ratio, C_r and the thermo-physical property-ratio, γ of the bath-additive system and the phase-change parameters, the Stefan number, S_{tb} of the bath material and the Stefan number, S_{ta} of the additive and the bath condition denoted by, the modified conduction factor, C_{ofm} . During the freezing and melting, the additive passes through the pre-melt heating, melting and post-melt heating. The time of freezing and melting is almost unaffected by change in S_{ta} or θ_{ab} , whereas the effect is significant in significant for variation in any of C_{ofm} , S_{tb} , and C_r .

2. MATHEMATICAL MODEL

To evolve a mathematical model for the freezing and melting of a bath material around a low melting temperature cylindrical additive, it is taken initially at a uniform temperature, T_{ai} less than its melting temperature, T_{am} ($T_{ai} < T_{am}$), and is plunged in a hot melt bath maintained at a constant temperature, T_b higher than the freezing temperature of the bath material, T_{bm} ($T_b > T_{bm}$). Instantly, the bath material begins to freeze around the cylindrical additive, the interface formed between additive and the freezing layer arrives at an equilibrium temperature, T_e , Figure 1.

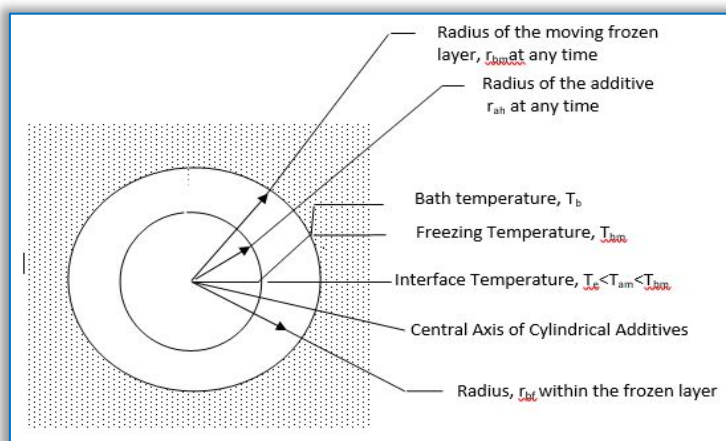


Figure 1: Schematic of Freezing and Melting of Bath Material onto a Low Melting Temperature Additive with pre-melt Heating of the Additive

The temperature T_e , lies between the initial temperature of the additive and freezing temperature of the bath material, ($T_e < T_{am} < T_e < T_{bm}$). Moreover, this event sets up a temperature field in the additive-bath system represented by $T_b > T_{bm} > T_e > T_{am} > T_{ai}$. It is shown in Figure 1. With passing of the time, the frozen layer grows in thickness so long as the heat conducted to the additive is more than the convective heat available from the bath. The excess conductive heat is provided by the latent heat of fusion evolved due to freezing of the bath material onto the additive. Once the conductive heat becomes equal to the bath convective heat, the growth of the frozen layer stops. After this time, the bath convective heat is greater than the conductive heat due to which the excess convective heat melts completely the frozen layer exposing the additive at the freezing temperature T_{bm} of the bath material. This situation is assumed to be controlled by conjugated transient heat conduction. The non-dimensional integral form of this heat conduction equation governing axi-symmetry freezing of the bath material onto the additive can be written as

$$\left[\frac{d}{d\tau} \int_{C_r}^{R_{bm}} R_{bf} \theta_{bf} dR_{bf} - [R_{bf} \theta_{bf}]_{R_{bf}=R_{bm}} \frac{dR_{bm}}{d\tau} + [R_{bf} \theta_{bf}]_{R_{bf}=C_r} \frac{dC_r}{d\tau} \right] = R_{bf} \frac{\partial \theta_{bf}}{\partial R_{bf}} \Big|_{R_{bf}=R_{bm}} - R_{bf} \frac{\partial \theta_{bf}}{\partial R_{bf}} \Big|_{R_{bf}=C_r}, C_r < R_{bf} < R_{bm}, \tau > 0 \quad (1)$$

From physical point of view, the first term of the right side of Eq.(1) indicates the rate of heat conduction to the freezing layer from the bath at $R_{af} = R_{bm}$ and the second term of the right side provides the rate of heat conducted to the additive through the interface formed between the additive and freezing layer at $R_{af} = C_r$. The difference of these two provides the net rise of the internal energy of the frozen layer denoted by the left side of Eq.(1). Its first term signifies the rate of increase in thermal energy whereas the combination of the second and third terms corresponds to the rate of internal thermal energy available due to increase in the frozen layer thickness onto the additive.

Its associated initial and boundary conditions are

$$\theta_{bf} = \theta_b, R_{bm} = C_r, \tau = 0 \quad (2)$$

$$\theta_{bf} = \theta_e > 0, R_{bf} = C_r, \tau > 0 \quad (3)$$

$$\frac{\partial \theta_{bf}}{\partial R_{bf}} = \frac{1}{\gamma C_{of}} + \frac{1}{S_{tb}} \frac{dR_{bm}}{d\tau}, \theta_{bf} = 1, R_{bf} = R_{bm}, \tau > 0 \quad (4)$$

As described above, this temperature, T_e of the interface rises from the initial temperature T_{ai} of the additive to the freezing temperature, T_{bm} , of the bath material. This additive is a solid cylinder of large length, l_a and small radius, r_{oa} and its thermal resistance is negligible in comparison with the thermal resistance of the bath convective heat along with that of the growing frozen layer. This situation makes the Biot number, B_i , a ratio between the additive thermal resistance and the thermal resistance of the bath comprising of the thermal resistance of the bath convective heat and the frozen layer becomes less than 0.1 ($B_i \leq 0.1$). This feature permits the establishment of a uniform temperature in the entire cylinder, which is exactly the same as the interface temperature, T_e , between the freezing layer and the additive. It makes the additive act as a lump [24,25]. With elapse of time, this temperature, T_e rises from T_{ai} to T_{bm} , and as explained earlier the frozen layer grows to a maximum thickness and then melts completely. During this time due to rise in temperature of the additive from T_{ai} to T_{bm} the additive undergoes through following three different events.

— **Case-I: Pre-melt Heating of the Additive**

In the first event, the temperature of the additive rises from its initial temperature T_{ai} to its melting temperature, T_{am} , and only heating of the additive takes place. It is recognised as pre melt heating and estimated once an energy balance between the increase in the thermal energy of the additive (lump) and the heat supplied from the bath through the frozen layer onto the lump is applied. It leads to

$$d\theta_a / d\tau = -2Q_{an} / \gamma, \tau > 0 \quad (5)$$

Its initial condition is given by

$$\theta_a = \theta_e = 0, 0 < R_{an} < 1, \tau = 0 \quad (6)$$

During the time of this event, the frozen layer of the bath material developed onto the additive is represented by $R_{bf} = R_{bh}$ and can be obtained from Eq.(1).

— **Case-II: Melting of the Additive at its Melting Temperature**

The second event corresponds to only melting of the lump after it attains its melting temperature, ($T_{am} < T_{bm}$) at time $\tau = \tau_{ah}$ in case-I. During this melting, the lump temperature remains at its melting temperature. In such an event, the energy balance between the heat conducted to the lump and the heat required to melt it completely can be cast as

$$-Q_{an} \Delta\tau = \gamma / 2S_{ta}, \tau > \tau_{ah} \quad (7)$$

Its initial condition is

$$\theta_a = \theta_e = \theta_{ab}, \tau = \tau_{ah} \quad (8)$$

Here, $\Delta\tau = \tau_{acm} - \tau_{ah}$ with τ_{acm} denoting the time at which the lump completely melts. The corresponding frozen layer of the bath material grown onto the lump is expressed by $R_{bf} = R_{bcm}$ and is still estimated from Eq.(1).

— **Case-III: Post melt Heating of the Additive**

In the third and last event, beyond the time τ_{acm} , the melt lump gets heated from the convective heat coming from the bath through the frozen layer, raising its melting temperature, T_{am} to the freezing temperature, T_{bm}

of the bath material whereas the frozen layer grows to its maximum thickness ($R_{bf} = R_{bmx}$) at time $\tau = \tau_{max} > \tau_{acm}$. An energy balance to this event with initial condition gives

$$d\theta_a/d\tau = -2Q_{an}/\gamma, \quad \theta_a = \theta_e = \theta_{ab}, \quad \tau > \tau_{acm} \quad (9)$$

$$\theta_a = \theta_e = \theta_{ab}, \quad \tau = \tau_{acm} > \tau_{ah} > 0 \quad (10)$$

Note that at the time $\tau = \tau_{max}$ the interface temperature and the freezing front temperature of the frozen layer of the bath material becomes at the melting temperature of the bath material. It makes the entire thickness of the frozen layer at the bath material melting temperature, T_{bm} . After this happening the bath convective heat only melts the frozen layer till it completely melts exposing the additive melt at the freezing temperature T_{bm} of the bath material. This melt then immediately assimilates in the melt bath making the melt of desired composition. Applying an energy balance between the rate of the melting of the frozen layer and bath convective heat that melts leads to

$$-\frac{1}{S_{tb}} \frac{dR_{bf}}{d\tau} = \frac{1}{\gamma C_{of}} = \frac{1}{C_{ofm}} \quad \tau > \tau_{max} \quad (11)$$

The conjugating conditions at the interface between the freezing bath material and the additive are

$$\partial\theta_{bf}/\partial R_{bf} = -Q_{an}/\gamma, \quad R_{bf} = C_r, \quad R_a = 1 \quad (12)$$

and

$$\theta_{bf} = \theta_a = \theta_e, \quad R_{bm} = C_r, \quad R_a = 1 \quad (13)$$

It is noted that θ_e remains within $\theta_e \leq \theta_{ab}$, $\theta_e = \theta_{ab}$, and $\theta_{ab} < \theta_e \leq 1$, respectively, for Case-I, Case-II and Case-III.

The model just evolved indicates that the freezing and melting of the bath material around the negligible thermal resistance additive of low melting temperature is controlled by independent non-dimensional parameters; the property-ratio, γ , the melting temperature-ratio, θ_{ab} , and the heat capacity-ratio, C_r of the additive-bath system, the Stefan number of the bath material, S_{tb} and that of the additive, S_{ta} and the conduction factor, C_{of} .

3. SOLUTIONS

Examination of the model comprising of Eqs.(1) to (13) reveals that the current event is mathematically non-linear owing to the phase-change moving boundary, Eq.(4) of the freezing bath material and Eq.(7) of the melting of the additive and coupled because of conjugating conditions, Eqs.(12) and (13). These features forbid its closed-form solutions when exact analyses of the literature are applied. In such a situation semi-analytical methods become suitable. Since an integral method, one of these employed in the recent past, gave closed-form solutions for several phase-change problems [26-28] or reduced such problems to first order ordinary differential equations [14,15,29] for which it did not yield closed-form solutions. Runge-Kutta method is often resorted to obtain numerical solutions.

— Solution for Case I: pre-melt heating of the additive

In view of the above, Eq.(1) regulating the freezing and melting of the bath material onto the additive has already been cast in an integral form which can be reduced to

$$\left[\frac{d}{d\tau} \int_{C_r}^{R_{bm}} R_{bf} \theta_{bf} dR_{bf} - R_{bm} \frac{dR_{bm}}{d\tau} \right] = R_{bf} \frac{\partial\theta_{bf}}{\partial R_{bf}} \Big|_{R_{bf}=R_{bm}} - R_{bf} \frac{\partial\theta_{bf}}{\partial R_{bf}} \Big|_{R_{bf}=C_r} \quad (14)$$

once Eqs. (3) and (4) are employed.

To solve this equation, prescription of temperature distribution within the frozen layer is required. A linear temperature profile of the following form is taken.

$$\theta_{bf} - \theta_e + (1 - \theta_e) \left(\frac{R_{bf} - C_r}{R_{bm} - C_r} \right) \quad (15)$$

It satisfies the boundary conditions, Eqs. (3) and (4). Its choice is realistic due to giving accurate results for the analogous phase-change problems [14,26-28] in the past studies. Applying Eqs.(4) and (15), Eq.(14) leads to

$$\frac{d}{d\tau} \left[\frac{\theta_e}{2} (R_{bm}^2 - C_r^2) + (1 - \theta_e) \left\{ \frac{1}{2} R_{bm} (R_{bm} - C_r) - \frac{1}{6} (R_{bm} - C_r)^2 \right\} - \frac{1}{2} R_{bm}^2 \right] = \frac{R_{bm}}{\gamma C_{of}} + \frac{1}{S_{tb}} R_{bm} \frac{dR_{bm}}{d\tau} - \frac{C_r (1 - \theta_e)}{R_{bm} - C_r} \quad (16)$$

Using Eqs.(12) and (15), Eq.(5) related to heating of the additive becomes

$$(R_{bm} - C_r) \frac{d\theta_e}{d\tau} + 2(\theta_e - 1) = 0 \quad (17)$$

when Eq.(15) is employed, Eqs.(16) and (18) are coupled due to presence of both R_{bm} and θ_e in them and their examination indicates that they do not lead to closed form solutions. Owing to this, they are arranged in terms of $\frac{dR_{bm}}{d\tau}$ and $\frac{d\theta_e}{d\tau}$ Eq.(16) then becomes

$$\left[A_1(\theta_e - 1) - \frac{R_{bm}}{S_{tb}} \right] \frac{dR_{bm}}{d\tau} + A_2 \frac{d\theta_e}{d\tau} = \frac{R_{bm}}{\gamma C_{of}} + \frac{C_r(\theta_e - 1)}{R_{bm} - C_r} \quad (18)$$

Here, $A_1 = \frac{C_r}{2} + \frac{1}{3}(R_{bm} - C_r)$, $A_2 = \frac{1}{2}C_r(R_{bm} - C_r) + \frac{1}{6}(R_{bm} - C_r)^2$

Using Eq. (17) Eq. (18) changes to

$$C_{ofm}(R_{bm} - C_r) \left[(\theta_e - 1)A_1 - \frac{R_{bm}}{S_{tb}} \right] \frac{dR_{bm}}{d\tau} = R_{bm}(R_{bm} - C_r) + C_{ofm}(\theta_e - 1)(C_r + 2A_2) \quad (19)$$

Eqs.(17) and (19) form an initial value problem having initial conditions $\theta_e = 0$, $R_{bm} = C_r$ at $\tau = 0$. These equations neither give closed-form solutions using any analytical methods nor get their solutions initiated owing to giving infinite value, ∞ at the initial conditions when the Runge-Kutta method is employed. To overcome this difficulty, series solutions for small times in the neighbourhood of time, $\tau \rightarrow 0$, i.e. ($\tau = 10^{-6}$), are resorted to obtain the starting values of θ_e and R_{bm} . These values are then employed as initial values in the Runge-Kutta method. It now gives numerical solutions that are calculated for all times.

— Series Solutions for Small times

To obtain the series solutions for small times that lie in the neighbourhood of the initial time $\tau = 0$, the series solutions for R_{bm} and θ_e can be respectively written as

$$R_{bm} = \sum a_i \tau^{i/2} \quad (20)$$

$$\theta_e = \sum b_i \tau^{i/2}, \quad i=0,1,2,\dots,n \quad (21)$$

are assumed. They fulfil the initial condition $\theta_e = 0$, $R_{bm} = C_r$ at $\tau = 0$. These give $a_0 = C_r$, and $b_0 = 0$. To facilitate the determination of other co-efficient of Eqs. (20) and (21), they are employed in Eqs. (17) and (18) giving

$$a_1 = \pm 2 \sqrt{\frac{S_{tb}}{2 + S_{tb}}}, \quad b_1 = \pm 2 \sqrt{\frac{2 + S_{tb}}{S_{tb}}}$$

$$a_2 = \left[\frac{4}{3} \left(C_{ofm} C_r - C_r - \frac{2}{3} C_{ofm} \right) S_{tb}^2 - \frac{8}{3} (C_r - C_{ofm}) S_{tb} - \frac{16}{3} C_{ofm} C_r \right] / C_{ofm} C_r (2 + S_{tb})^2$$

$$b_2 = \left[\frac{2}{3} \left(C_r + \frac{2}{3} C_{ofm} - 4 C_{ofm} C_r \right) S_{tb}^2 + \left(\frac{4}{3} C_{ofm} - 8 C_{ofm} + \frac{4}{3} C_r \right) S_{tb} - \frac{16}{3} C_{ofm} C_r \right] / C_{ofm} C_r S_{tb} (2 + S_{tb})$$

$$a_3 = \left[\frac{1}{9} \left(-\frac{10}{3} C_{ofm} C_r + 2 C_r^2 - \frac{26}{3} C_{ofm}^2 C_r - 22 C_r^2 C_{ofm} + \frac{80}{9} C_{ofm}^2 + 2 C_{ofm}^2 C_r^2 \right) S_{tb}^4 \right. \\ \left. + \frac{1}{9} \left(-36 C_{ofm}^2 C_r^2 - 98 C_r^2 C_{ofm} + \frac{4}{3} C_{ofm} C_r + \frac{160}{3} C_{ofm}^2 + 8 C_r^2 - 44 C_{ofm}^2 C_r \right) S_{tb}^3 \right. \\ \left. + \frac{1}{9} \left(-80 C_{ofm}^2 - 128 C_r^2 C_{ofm} - 160 C_{ofm}^2 C_r + 16 C_{ofm} C_r - \frac{4}{3} C_{ofm}^2 C_r + 8 C_r^2 \right) S_{tb}^2 \right. \\ \left. + \frac{1}{9} \left(240 C_{ofm}^2 C_r - 40 C_{ofm} C_r^2 - 88 C_{ofm}^2 C_r \right) S_{tb} + \frac{1}{9} \left(32 C_{ofm}^2 C_r^2 \right) \right] / \left[C_{ofm}^2 C_r^2 \left\{ S_{tb} (2 + S_{tb})^{\frac{1}{2}} \right\} (2 + S_{tb})^3 \right]$$

$$b_3 = \left[\frac{1}{9} \left(-10 C_{ofm} C_r^2 + 2 C_r^2 - \frac{26}{3} C_{ofm}^2 C_r - \frac{16}{9} C_{ofm}^2 + 26 C_{ofm}^2 C_r^2 + \frac{14}{3} C_{ofm} C_r \right) S_{tb}^4 \right. \\ \left. + \frac{1}{9} \left(156 C_{ofm}^2 C_r^2 - 50 C_r^2 C_{ofm} + \frac{52}{3} C_{ofm} C_r - \frac{32}{3} C_{ofm}^2 + 8 C_r^2 - 52 C_{ofm}^2 C_r \right) S_{tb}^3 \right]$$

$$\begin{aligned}
 & + \frac{1}{9} \left(8C_r^2 + 320C_r^2 C_{ofm}^2 - 16C_{ofm}^2 + 16C_{ofm} C_r - \frac{340}{3} C_{ofm}^2 C_r - 80C_{ofm} C_r^2 \right) S_{tb}^2 \\
 & + \frac{1}{9} \left(240C_{ofm}^2 C_r^2 - 40C_{ofm} C_r^2 - 88C_{ofm}^2 C_r \right) S_{tb} + \frac{1}{9} \left(32C_{ofm}^2 C_r^2 \right) \left/ \left[C_r^2 S_{tb} \left\{ S_{tb} (2 + S_{tb})^{\frac{1}{2}} \right\} (2 + S_{tb})^2 \right] \right.
 \end{aligned}$$

Note that the Mat Lab facilitates to provide above expressions.

— Numerical solutions for all times:

As explained earlier, the starting values for R_{bm} and θ_e in the vicinity of $\tau \rightarrow 0$, i.e. ($\tau = 10^{-6}$), are found from the above series solutions They are then used in Runge-Kutta method to estimate R_{bm} and θ_e from Eqs. (17) and (18) until the time at which θ_e attains the melting temperature, θ_{ab} of the additive. The solutions so obtained indicate that the rate of rise of the additive temperature, θ_e is faster than the growth of the frozen layer, due to which the additive attains its melting temperature, θ_{ab} before the growing frozen layer reaching its maximum thickness. At this time, τ_{ah} the developed frozen layer is denoted by R_{bh} .

— Solutions for Case-II, Melting of the additive at its Melting Temperature

Beyond this time, τ_{ah} the additive begins to melt till it melts completely at its melting temperature. $\theta_e = \theta_{ab}$. The frozen layer onto the additive, however, continues to grow to attain R_{bcm} at the time τ_{acm} of complete melting

of additive. Here, $\frac{d\theta_e}{d\tau} = \frac{d\theta_{ab}}{d\tau} = 0$ and $\theta_e = \theta_{ab}$. Their substitution in Eq. (18) leads to

$$\left[(\theta_{ab} - 1)A_1 - \frac{R_{bm}}{S_{tb}} \right] \frac{dR_{bm}}{d\tau} = \frac{R_{bm}}{C_{ofm}} + \frac{C_r(\theta_{ab} - 1)}{R_{bm} C_r} = \frac{R_{bm}(R_{bm} - C_r) + C_r C_{ofm}(\theta_{ab} - 1)}{C_{ofm}(R_{bm} - C_r)} \quad (22)$$

whereas the initial condition for this situation becomes

$$R_{bm} = R_{bmh}, \tau = \tau_{ah} \quad (23)$$

The melting of the additive is obtained by equating the heat conducted to the additive through the interface from the frozen layer Eq.(12), and the heat absorbed as the latent heat of fusion by the additive. It gives

$$-\frac{Q_{an}}{\gamma} = \frac{1}{2S_{ta}(\tau - \tau_{ah})} = \frac{\partial \theta_{bf}}{\partial R_{bf}} \Big|_{R_{bf}=C_r} \quad (24)$$

Employing Eq. (15) with $\theta_e = \theta_{ab}$ Eq.(24) is transformed to

$$2S_{ta}(\tau - \tau_{ah}) = (1 - \theta_e)/(R_{bm} - C_r) \quad (25)$$

In this situation, Eq. (22) for the freezing and melting readily gives a closed-form solution. Rearranging this Eq.(22) gives

$$\frac{d\tau}{dR_{bm}} = \frac{\gamma C_{ofm} (R_{bm} - C_r) [(\theta_{ab} - 1) \left\{ \frac{C_r}{2} + \frac{1}{3} (R_{bm} - C_r) \right\} - \frac{R_{bm}}{S_{tb}}]}{R_{bm} (R_{bm} - C_r) + \gamma C_{ofm} C_r (\theta_{ab} - 1)} \quad (26)$$

Assuming $R_{bm}^* = R_{bm} - C_r$, Eq.(26) is recast as

$$\frac{d\tau}{dR_{bm}^*} = \frac{A_3 R_{bm}^{*2}}{R_{bm}^{*2} + C_r R_{bm}^* + A_5} + \frac{A_4 R_{bm}^*}{R_{bm}^{*2} + C_r R_{bm}^* + A_5} \quad (27)$$

It yields a closed-form solution that satisfies the initial condition of this occurrence

$$\tau = \tau_{ah}, \quad R_{bm} = R_{bmh} \quad (28)$$

$$\tau - \tau_{ah} = A_3 (R_{bm}^* - R_{bmh}^*) - A_8 \ln \left(\frac{R_{bm}^{*2} + C_r R_{bm}^* + A_5}{R_{bmh}^{*2} + C_r R_{bmh}^* + A_5} \right) + A_9 \ln \left(\left(\frac{2R_{bm}^* + C_r - A_6}{2R_{bmh}^* + C_r - A_6} \right) \left(\frac{2R_{bm}^* + C_r + A_6}{2R_{bmh}^* + C_r + A_6} \right) \right) \quad (29)$$

where,

$$\begin{aligned}
 A_3 &= \frac{1}{3} C_{ofm} (\theta_{ab} - 1) - \frac{C_{ofm}}{S_{tb}}, \quad A_4 = \frac{1}{2} C_{ofm} C_r (\theta_{ab} - 1) - \frac{C_{ofm} C_r}{S_{tb}}, \quad A_5 = C_{ofm} C_r (\theta_{ab} - 1), \\
 A_6 &= \sqrt{C_r^2 - 4A_5}, \quad A_7 = C_r^2 - 2A_5, \quad A_8 = \frac{A_3 C_r - A_4}{2}, \quad A_9 = \frac{A_3 A_7 - A_4 C_r}{2A_6}
 \end{aligned}$$

Eq. (29) provides the behaviour of the freezing and melting of the bath material during which the additive melts at its melting temperature, θ_{ab} . At the time of completion of the melting of the additive denoted by $\tau =$

τ_{am} , the frozen layer thickness R_{bm} increases from R_{bh} to R_{bmm} . The behaviour of R_{bm} in the range of $R_{bh} \leq R_{bm} \leq R_{bmm}$ can be obtained once Eqs. (25) and (29) are employed. It gives

$$\frac{1}{2S_{ta}(1-\theta_{ab})} = \frac{1}{R_{bm}^*} \left[A_3(R_{bm}^* - R_{bmh}^*) - A_8 \ln \left(\frac{R_{bm}^{*2} + C_r R_{bm}^* + A_5}{R_{bmh}^{*2} + C_r R_{bmh}^* + A_5} \right) + A_9 \ln \left(\left(\frac{2R_{bm}^* + C_r - A_6}{2R_{bmh}^* + C_r - A_6} \right) \left(\frac{2R_{bmh}^* + C_r + A_6}{2R_{bm}^* + C_r + A_6} \right) \right) \right] \quad (30)$$

For prescribed values of S_{ta} , S_{tb} , θ_{ab} , γ , C_r Eq. (30) readily gives the value of $R_{bm}^* = R_{bmm}^* = R_{bmm} - C_r$, when the additive completely melts.

— Solution for Case III: Post Melt Heating of the Additive melt

After the time of above occurrence the melt temperature, θ_e increases from θ_{ab} to the freezing temperature of the bath material ($\theta_e = 1$). During this period the melt only gets heated. It is still governed by Eq.(17) whereas Eq. (18) regulates the freezing and melting of the bath material onto the additive for $\theta_e > \theta_{ab}$ and $R_{bm} > R_{bmm}$ Combination of these two equations, Eqs. (17) and (18) subjected to initial conditions

$$\theta_e = \theta_{ab}, R_{bm}^* = R_{bmm}^*, \tau = \tau_{am} \quad (31)$$

leads to

$$\frac{dR_{bm}}{d\tau} = \frac{R_{bm}(R_{bm} - C_r) + \gamma C_{of}(\theta_e - 1)(C_r + 2A_2)}{(R_{bm} - C_r) \left\{ A_1(\theta_e - 1) - \frac{R_{bm}}{S_{tb}} \right\} C_{ofm}} \quad (32)$$

Note that Eqs. (17) and (32) form a simultaneous first order ordinary differential equations in an independent variable τ , the solutions of which can be immediately found using Runge-Kutta method. In this case also, the rate of rise of the additive melt temperature is much faster than the further growth of the frozen layer, resulting in the interface temperature, θ_e reaching earlier the freezing temperature of the bath material ($\theta_e=1$). As growing frozen layer front in contact with bath is already at the bath material freezing temperature, the entire frozen layer becomes at this freezing temperature ($\theta_e=1$) due to which no heat is conducted through such a layer resulting in ceasing the further growth of frozen layer. In this situation, the frozen layer attains the maximum thickness. Beyond this happening the bath convective heat is utilized in only melting the frozen layer till the frozen layer completely melts. Applying an energy balance to such an event between the melting of the frozen layer and the bath convective heat enabling this layer to melt is given by

$$-\frac{1}{S_{tb}} \frac{dR_{bm}}{d\tau} = B_{im}(\theta_b - 1) = \frac{1}{C_{ofm}} \quad (33)$$

It can also be readily derived from Eq. (24) when $\theta_e=1$ is substituted in it. The closed-form solution of Eq.(33) becomes

$$R_{bm} = R_{bmx} - \frac{S_{tb}}{C_{ofm}}(\tau - \tau_{max}) \quad (34)$$

which satisfies the boundary condition $\tau = \tau_{max}$ when $R_{bm} = R_{bmx}$, the thickness of maximum frozen layer Eq. (34) readily gives the total time, τ_t of freezing and melting once R_{bmx} becomes C_r , after melting the frozen layer. Their substitution in Eq.(34) leads to

$$\tau_t = \frac{C_{ofm}}{S_{tb}} R_{bmx}^* + \tau_{max}, \quad \text{where } R_{bmx}^* = R_{bmx} - C_r \quad (35)$$

4. VALIDATION

To validate the current problem, the bath convective heat is maintained at such a large value that it exceeds the requirement of additive conductive heat, resulting in no development of the frozen layer onto the additive rather only heating of the additive takes place. It makes this problem a classic problem [24,25] of unsteady state heating of the cylindrical solid additive of negligible thermal resistance subjected to convective heating from the bath. This vanishes of Eq.(16) and replaces the right hand side of Eq.(17) by the bath convective heat resulting in

$$d\theta_e/d\tau = B_i(\theta_b - \theta_e) \quad (36)$$

Its initial condition is

$$\theta_e = 0 \quad \tau = 0 \quad (37)$$

The solution of Eq. (42) satisfying Eq. (43) yields

$$(1 - (\theta_e / \theta_b)) = e^{-B_1 \tau} \quad (38)$$

It is exactly the same as that of the literature [24,25].

5. RESULTS AND DISCUSSIONS

The event of axi-symmetric freezing and melting of the bath material around a low melting temperature cylindrical additive soon after immersion of this additive in the bath is investigated, when the additive thermal resistance is negligible with respect to the thermal resistance of the bath including the frozen layer formed onto the additive. Its non-dimensional mathematical model of lump-integral form is devised. It enables to show this event dependence upon the non-dimensional independent parameters; the phase-change parameter, the Stefan number of the bath material, S_{tb} , and that of the additive, S_{ta} , the bath condition regulated by the modified conduction factor C_{ofm} , the property-ratio, γ , the heat capacity-ratio, C_r , and the melting temperature-ratio, θ_{ab} , of the additive-bath system. Their values for different additive-bath systems are presented in (TABLE 1). The Stefan number is the ratio between sensible heat and latent heat of fusion of the phase-change material. Its low value is indicative of high latent heat of fusion allowing the development of smaller thickness of the frozen layer of the bath material onto the additive for the same convective heat supplied by the bath or enabling to melt smaller thickness of the additive. The melting temperature-ratio, $\theta_{ab} < 1$ of the additive denotes the additive melting temperature lower than that of the bath material. It causes both heating and melting of the additive. C_r , the heat capacity-ratio is the ratio of the heat capacity of the bath material and the heat capacity of the additive. $C_r > 1$ represents large sensible heat release by the freezing layer with respect to that in the additive.

Table – 1: Based on thermo physical properties of the Steel bath [3]

Additive	Thermo-physical properties of low melting temperature cylindrical solid additive [34] [$T_{ai}=293K(20^\circ C)$, $r_o=0.01m$]					Non-dimensional parameters			
	T_{am} [K($^\circ C$)]	C_{pa} J/KgK	ρ_a Kg/m ³	L_a J/Kg	K_a^* W/mK	S_{ta}	θ_{ab}	C_r	C_{ofm}
Magnesium	923(650)	1024	1740	376830	156	4.106	0.417	2.984	136.133
Zink	693(420)	389	7140	100860	116	5.827	0.264	1.914	87.33
Lead	600(327)	130	11373	29100	35.1	6.75	0.203	2.664	164.057

$$T_b = 1873K(1600^\circ C), T_{bm} = 1804K(1531^\circ C), C_b = 0.69KJ/KgK, L_{bm} = 277000 J/Kg,$$

$$K_{bm} = 29.3W/mK, \rho_{bm} = 7820Kg/m^3, S_{tb} = 3.71, h = 1000 W/m^2K.$$

Due to this the total heat available from the bath side which is sum of the bath convective heat, and release of sensible heat, increases resulting in decrease in requirement of less latent heat of fusion to meet the conductive heat needed by the additive. It yields in growth of lesser thickness of the frozen layer, Figure 8. The modified conduction factor, C_{ofm} is the product of the property-ratio and the conduction factor, C_{of} ($C_{ofm} = \gamma C_{of}$). This C_{of} is defined as the ratio of heat conducted to the additive due to difference of the freezing temperature of the bath material and the initial temperature of the additive and the convective heat given by the bath. It lies between 0 and ∞ ($0 \leq C_{of} \leq \infty$) $C_{of} \rightarrow 0$ pertains to no heat conduction to the additive. Owing to this, the freezing does not occur. It results in absence of the freezing and melting. Also, $C_{of} \rightarrow 0$ can be attained in case the bath is made highly agitated enabling to give extremely high heat transfer coefficient, $h \rightarrow \infty$, and, in turn, high bath convective heat, $h(T_b - T_{bf})$. It balances the heat conducted to the additive. Consequently, no freezing of the bath material onto the additive takes place. $C_{of} \rightarrow \infty$ corresponds to the absence of the bath convective heat owing to which the heat conducted to the additive is met by the latent heat of fusion generated by only freezing of the bath material onto the additive. These suggest that the time of undesirable freezing and melting can be reduced to a negligible value once the conduction factor is brought to almost zero value ($C_{of} \rightarrow 0$), for an additive-bath system. It is attained by making the bath highly agitated.

Figure 2 exhibits the time-variant freezing and melting of the bath material onto the low melting temperature additive, and the rise in the temperature of the additive during the freezing and melting for different values of the modified conduction factor, C_{ofm} with S_{tb} , S_{ta} , C_r and θ_{ab} assumed to be parameters. Figure 4 corresponds to these behaviours but for various values of the Stefan number S_{tb} of the bath material. C_{ofm} , S_{ta} , C_r and θ_{ab} are taken as parameters. Depicted in Figure 6 are these behaviours for different Stefan number, S_{ta} of the additive when S_{tb} , C_{ofm} , C_r and θ_{ab} are considered as parameters. These behaviours are plotted in Figure 8 for various values of the melting temperature ratio θ_{ab} in case of specified S_{ta} , S_{tb} , C_{ofm} and C_r whereas in Figure 10 they are for different C_r , when S_{ta} , S_{tb} , θ_{ab} and C_{ofm} act as parameters. All these figures show unique behaviour of the freezing and melting in that the frozen layer up to its maximum thickness is parabolic, whereas its melting follows a linear behaviour and takes more time to melt them than that of the

freezing time. It is in contrast with the large time taken for the development of the frozen layer of the bath material onto the high melting temperature additive of negligible thermal resistance [14]. The associated temperature of the additive also builds-up fast to reach its melting temperature. With passing of the time, the melting temperature remains unaltered till the additive absorbs heat coming from the bath through the contact interface equal to its latent heat of fusion in order to convert the solid phase of the additive to the melt phase of the additive at its melting temperature. After this, the melt of the additive temperature rises to the freezing temperature of the bath material and then it remains at this freezing temperature until the frozen layer completely melts exposing the additive in the melt state which immediately mixes and assimilates in the bath.

— Influence of modified conduction factor, C_{ofm}

Figure 2 relates to the behaviour of the freezing and melting of the bath material around the additive with time for different C_{ofm} . The S_{ta} , S_{tb} , θ_{ab} , and C_r act as parameters. As stated earlier, for any C_{ofm} , the freezing region is parabolic whereas the melting zone is linear, but as C_{ofm} decreases its size reduces diminishing the maximum frozen layer thickness developed, its time of formation, the total time of the freezing and melting, and the time of melting of the frozen layer developed.

The corresponding rise in the temperature in the additive to the freezing temperature of the bath material also takes place at reduced time. Physically, this behaviour seems to be true since decreasing C_{ofm} increases the bath agitation and the associated bath convection. As the heat conducted to the additive is balanced by the sum of the convective heat of the bath and the latent heat of fusion generated by the freezing of the bath material onto the additive, the reduced C_{ofm} and, in turn, increased bath convection diminishes the requirement of the latent heat of fusion resulting in the formation of smaller thickness of the frozen layer. Its melting time becomes less and the time of the freezing and melting is also less, Figure 2. In this reduced time, the rise in temperature of the additive to attain freezing temperature of bath material is faster, inset of Figure 2. The graphs in Figure 3 relate to the modified conduction factor, C_{ofm} variant maximum frozen layer thickness grown, R_{bmx}^* , its time of development, τ_{max} and the total time of freezing and melting, τ_t . They indicate that R_{bmx}^* and its time of development τ_{max} vary linearly with increase in the modified conduction factor, C_{ofm} for prescribed values of S_{tb} , θ_{ab} , C_r and S_{ta} . But the total time of the freezing and melting increases fast once C_{ofm} is allowed to increase.

— Effect of the Stefan number of the bath material, S_{tb}

Shown in Figure 4 are the time-variant freezing and melting of the bath material onto the additive, and the temperature build-up in the additive for various S_{tb} with S_{ta} , C_{ofm} , C_r and θ_{ab} , behaving as parameters. Their behaviour is similar to those exhibited in Figure 2 for any S_{tb} , but unlike the appreciable change in the maximum frozen layer thickness, its time of formation, its time of melting of the frozen layer and the time of the freezing and melting for change of C_{ofm} from 50 to 150, there is negligible change in the maximum thickness of the frozen layer grown and its time of development, as S_{tb} rises from 2 to 4. However, in this range of S_{tb} the time of melting of the frozen layer and time of the freezing and melting increase much once S_{tb} decreases from 4 to 2. This is true since decrease in S_{tb} increases the latent heat of fusion of the bath material due to which the available bath convective heat melts the frozen layer slowly in comparison with that of the low latent heat

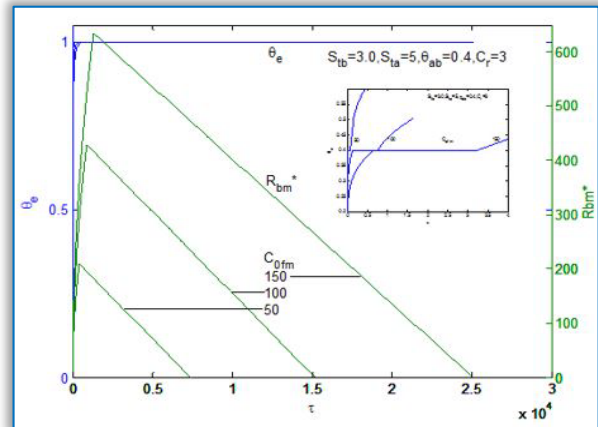


Figure 2: Time dependent freezing and melting of the bath material onto the low melting temperature cylindrical additive of negligible thermal resistance and the corresponding temperature rise in the additive for different modified conduction factors, C_{ofm} . S_{tb} , C_r , θ_{ab} and S_{ta} are taken as parameters. The inset relates to detail of temperature rise in the additive.

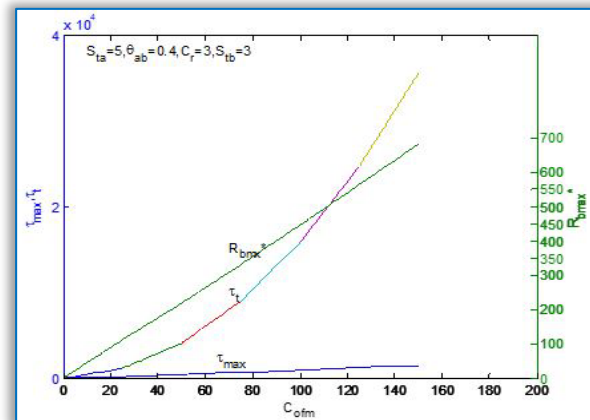


Figure 3: Variation of maximum frozen layer thickness, R_{bmx}^* , its growth time, τ_{max} and the total time τ_t , of freezing and melting of the bath material with modified conduction factors, C_{ofm} , for certain values of S_{ta} , θ_{ab} , C_r and S_{tb} .

of fusion of frozen layer. It results in increased time of the freezing and melting, Figure 4. Exhibited in Figure 5 are the maximum frozen layer developed, R_{bmx}^* , its time of growth, τ_{max} and the total time of the freezing and melting, τ_t with the Stefan number, S_{tb} of the bath material for given S_{ta} , θ_{ab} , C_r and C_{ofm} . The rise in R_{bmx}^* is linear with respect to S_{tb} but its time of development, τ_{max} is almost invariant with increase in S_{tb} . The total time of the freezing and melting, however, decreases once S_{tb} increases. It is true since increase in S_{tb} decreases the latent heat of fusion of the bath material allowing faster melting of the frozen layer by the same convective heat supplied from the bath resulting in reduction of the total time of freezing and melting.

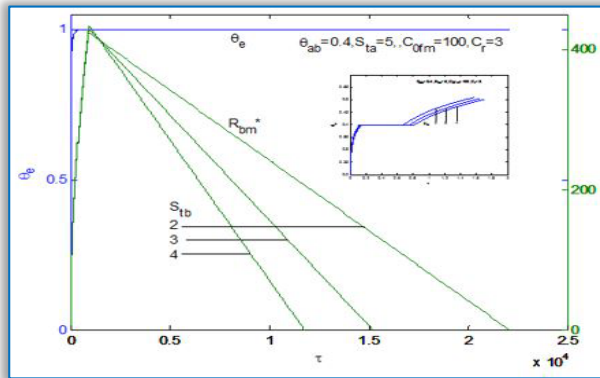


Figure 4: Time variant freezing and melting of the bath material onto the low melting temperature of negligible thermal resistance cylindrical additive and the corresponding build-up in the temperature in the additive for different Stefan number of melt bath material, S_{tb} . C_{ofm} , C_r , θ_{ab} and S_{ta} are taken as parameters. The inset exhibits the detail of the temperature rise in the additive.

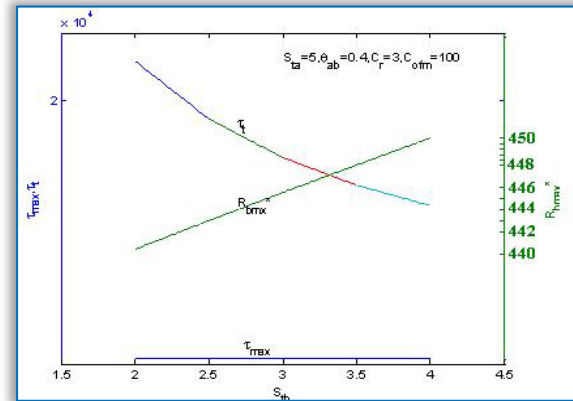


Figure 5: Stefan number, S_{tb} of the bath material variant maximum frozen layer thickness, R_{bmx}^* , its growth time τ_{max} and total time τ_t , of freezing and melting of the bath material for certain values of S_{ta} , θ_{ab} , C_r , and C_{ofm} .

— Effect of Heat Capacity -ratio, C_r :

Figure 6 is related to the freezing and melting of the bath material and the behaviour of the temperature in the additive with time for different heat capacity-ratio, C_r , S_{ta} , S_{tb} , θ_{ab} , and C_{ofm} behave as parameters. These graphs show similar behaviour as those appeared in Figure 4. However, it is observed that decreasing C_r increases the freezing and melting time, the growth of the maximum frozen layer thickness, its time of development and its time of melting. The associated rise in temperature to reach the melting temperature of the additive gets retarded, inset of Figure 6. Such findings are true since decrease in C_r reduces the heat capacity of the bath material.

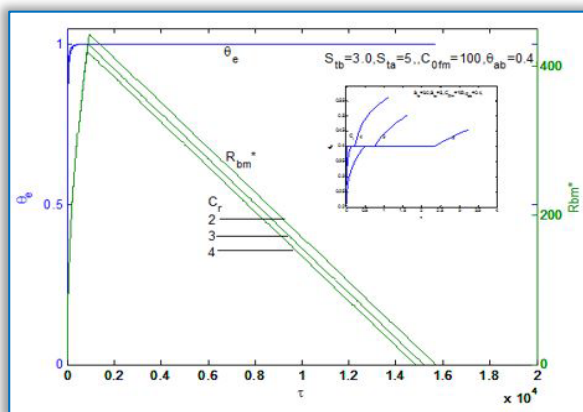


Figure 6: Time dependent freezing and melting of the bath material onto the low melting Temperature cylindrical solid additive of negligible thermal resistance and the corresponding rise in temperature of in the additive for different Capacity ratio, C_r , of additive-melt system. C_{ofm} , S_{tb} , θ_{ab} , and S_{ta} are considered as parameters. The inset provides the detail of temperature rise in the additive.

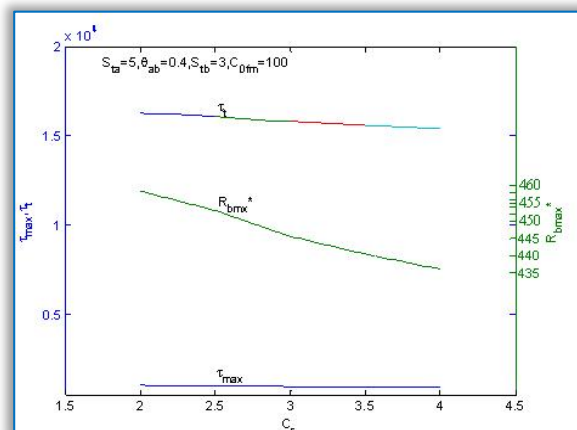


Figure 7: Variation of maximum frozen layer thickness, R_{bmx}^* , its growth time τ_{max} and total time τ_t , of freezing and melting of the bath material with different values of C_r of the additive-bath system for certain values of θ_{ab} , C_{ofm} , S_{ta} and S_{tb} .

It results in liberation of lesser sensible heat during the freezing of the bath material due to which availability of the total heat consisting of the sensible heat plus bath convective heat and latent heat of fusion released

due to freezing of the bath material becomes less and in order to meet the conductive heat requirement of the additive, more latent heat of fusion of the bath material is needed. It is compensated by the growth of the larger thickness of the frozen layer, Figure 6.

The heat capacity-ratio, C_r dependent maximum thickness of the frozen layer developed, R_{bmx}^* , its time of growth, τ_{max} and the total time of the freezing and melting τ_t are shown in Figure 7. In this case also, all of them are almost linear with respect to C_r but their values decrease once C_r increases from 2 to 4. However, decrease in R_{bmx}^* is faster. It is owing to fact that increase in C_r increases the heat capacity of the bath material and, in turn, the available heat from the bath side which is sum of the bath convective heat and the increased sensible heat. This results in requirement of less latent heat of fusion to compensate the conductive heat needed by the additive which is available due to growth of the smaller thickness of the frozen layer Figure 7.

— **Impact of the Stefan number of the additive S_{ta} :**

Figure 8 corresponds to the time-dependent freezing and melting of the bath material onto the additive and the associated rise in temperature of the additive in case of different S_{ta} , S_{tb} , θ_{ab} , C_r and C_{ofm} are assumed to be parameters. It is observed that the behaviour of the freezing and melting and the temperature of additive are similar to those of Figs. 2 and 4. However, irrespective of change in S_{ta} from 4 to 6, there is no change in the freezing and melting graph. It is possibly due to the fact that despite change in S_{ta} , the additive remains of the negligible thermal resistance causing no change in the freezing and melting graph for a given bath convective heat. But the corresponding interface temperature between the additive and frozen layer rises to the melting temperature of the additive faster, Figure 6 as S_{ta} increases from 4 to 6. It is due to the fact that decreasing S_{ta} reduces the latent heat of fusion of the additive and increases the availability of larger bath convective heat after compensating this latent heat. This permits the attainment of the melting temperature in the shorter time, inset of Figure 8. Figure 9 displayed S_{ta} variant the maximum frozen layer thickness, R_{bmx}^* , its time of growth, τ_{max} , and the total time of the freezing and melting, τ_t . It is observed that they are almost invariant as S_{ta} changes. It is true since the freezing and melting graph remains the same despite change in S_{ta} Figure 8.

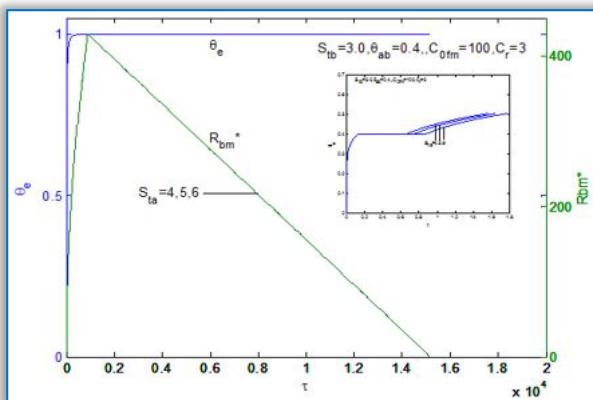


Figure 8: Behaviour of the freezing and melting of the bath material onto low melting temperature cylindrical additive of negligible thermal resistance and the corresponding rise in temperature of the additive with time for different Stefan number, S_{ta} of additive. C_{ofm} , C_r , θ_{ab} and S_{ta} are taken as parameters. The inset indicates the detail of additive temperature rise.

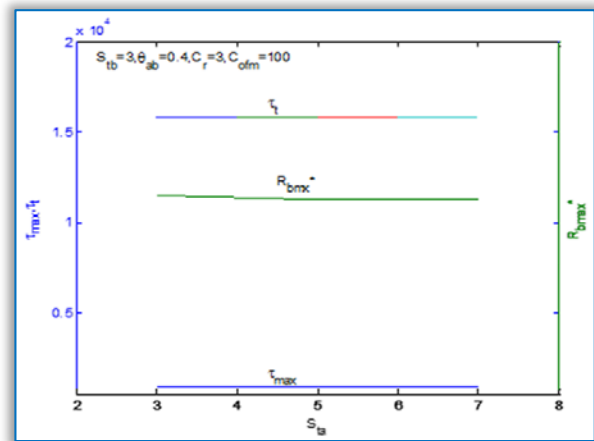


Figure 9: Stefan number, S_{ta} of the additive dependent the maximum frozen layer thickness, R_{bmx}^* , its growth time τ_{max} and total time τ_t , of freezing and melting of the bath material for certain values of S_{ta} , θ_{ab} , C_r and C_{ofm} .

— **Influence of melting temperature – ratio, θ_{ab} :**

In the Figure 10 are exhibited the freezing and melting of the bath material onto the additive and the temperature build-up in the additive with time for various melting temperature-ratio, θ_{ab} . S_{ta} , S_{tb} , C_{ofm} and C_r act as parameters. The freezing and melting feature is similar to that appeared in Figure 8. However, increasing θ_{ab} increases slightly, the maximum frozen layer thickness developed, its time of freezing, its time of melting and the total time of freezing and melting. This happens because increase in θ_{ab} increases the melting temperature of the additive and in order to raise this temperature, the available bath convective heat takes more time. This, in turn, causes the growth of the frozen layer of larger thickness taking more time to melt by the available bath convective heat. Figure 11 corresponds to plots of the maximum frozen layer thickness developed, R_{bmx}^* , its time of growth, τ_{max} , and the total time of the freezing and melting τ_t with respect to θ_{ab} . All of them increase almost linearly as θ_{ab} increases. Such a prediction is realistic since rise in θ_{ab} raises the melting temperature of the additive that requires more time for its attainment. In this increased time, the

growth of R_{bmax}^* , and melting time become larger for the available convective heat of the bath. Comparing the effect of either C_{ofm} or S_{tb} on these parameters namely R_{bmax}^* , τ_{max} and τ_t , the effect of θ_{ab} is insignificant.

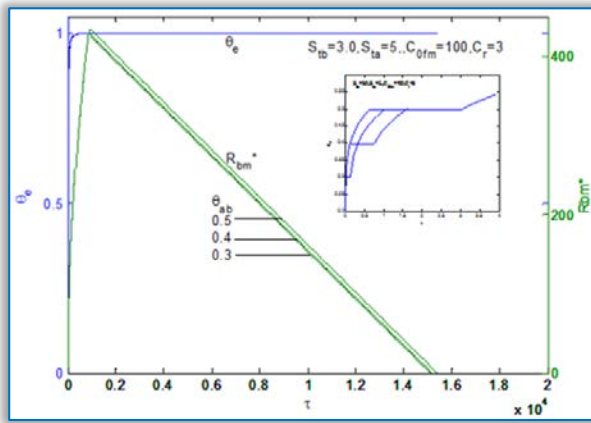


Figure 10: Time dependent freezing and melting of the bath material onto the low melting temperature and negligible thermal resistance cylindrical solid additive for different Stefan number, S_{ta} of the additive considering C_{ofm} , S_{tb} , C_r , and θ_{ab} are taken as parameters. The inset indicates corresponding temperature rise in the additive.

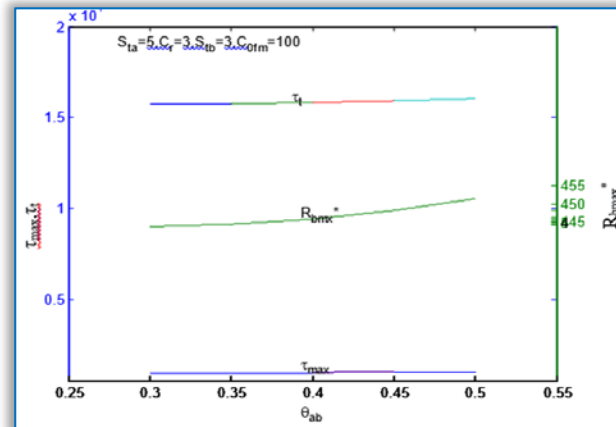


Figure 11: Behavior of maximum frozen layer thickness, R_{bmx}^* , its time of growth τ_{max} and total time τ_t , of freezing and melting of the bath material with Stefan number, S_{ta} of the additive for certain values of θ_{ab} , C_{ofm} , C_r and S_{tb} .

— Model Application to Industrial Practices

The solutions of the model just developed is applied to additives namely aluminium, magnesium and zinc often employed in steel manufacturing. It is observed from the Figure 12 that for the given bath condition, [Table-1] the zinc takes minimum time for the freezing and melting of the bath material onto it. It, in turn, takes minimum production time for the manufacture of steel.

6. CONCLUSIONS

During this event of unavoidable freezing and melting, the model indicates that the additive undergoes three phases denoted by the pre-melt heating, the melting of the additive at the melting temperature and post-melt heating. The pre-melt heating of the additive is regulated by C_{ofm} , S_{tb} and C_r whereas, additive melting and post-melt heating of the additive are controlled by S_{tb} , C_r , C_{ofm} , θ_{ab} and S_{ta} . The solutions of additive pre-melt and post-melt heating are in numerical form and that for the melting in closed-forms. The freezing and melting time is unaffected by change in S_{ta} of the additive whereas this time alters insignificantly due to change in either θ_{ab} or C_r . For a prescribed additive-bath system, unavoidable freezing and melting time and, in turn, production time can be reduced once C_{ofm} is decreased.

NOMENCLATURE

- B_i Biot number, hr_a/K_a
- B_{im} Modified Biot number, $(hr_a/K_a) * (K_a C_a / K_b C_b)$
- C heat capacity (ρC_p), $Jm^{-3} K^{-1}$
- C_{of} conduction factor, $1/\gamma B_{im}(\theta_b-1)$, $1/B_i(\theta_b-1)$,
- C_{ofm} modified conduction factor, $C_{of}(\theta_{ab}-1)$
- C_p specific heat, $(J Kg^{-1} K^{-1})$
- C_r heat capacity ratio, C_b/C_a
- h heat transfer coefficient, $Wm^{-2} K^{-1}$
- K thermal conductivity, $Wm^{-1} K^{-1}$
- L latent heat of fusion, JKg^{-1}
- r radius, m
- R_{ah} non-dimensional radius in the heat penetration region of the additive, (r_{ah}/r_a)
- R_{ai} non-dimensional radius of the heat penetration front in the additive at any time, (r_{ai}/r_a)
- R_{bf} non-dimensional radius within the frozen layer region, $(C_b r_{bf} / C_a r_a)$

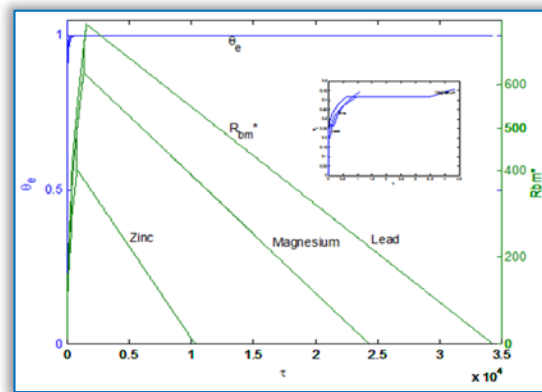


Figure 12: Time dependent freezing and melting of the bath material onto the low melting temperature and negligible thermal resistance cylindrical solid additive and associated temperature built-up in the additive often employed in steel manufacturing.

R_{bm}	non-dimensional radius of the frozen layer front at anytime, $(C_b r_{bm}/C_a r_a)$
St_a	Stefan number of the additive, $C_a(T_{bm}-T_{ai})/L_a \rho_a$
St_b	Stefan number of the bath material, $C_b(T_{bm}-T_{ai})/L_b \rho_b$
t	time, s
T	temperature, K
T_b	bulk temperature of the bath material, K
T_e	instant equilibrium temperature at the interface between the additive and the frozen layer, K

GREEK LETTERS

α	thermal diffusivity, $m^2 s^{-1}$
γ	property ratio, $(K_b C_b / K_a C_a)$
ρ	density, $(Kg m^{-3})$
θ	non-dimensional temperature, $(T - T_{ai} / T_{bm} - T_{ai})$
θ_{ab}	ratio of melting or freezing temperature of the additive that of the bath, $(T_{am} - T_{ai}) / (T_{bm} - T_{ai})$
τ	non-dimensional time, $(K_b C_b / C_a^2 r_0^2) t = \frac{\gamma \alpha_a t}{r_a^2}$

τ^* non-dimensional time per unit property ratio,

SUBSCRIPTS

a	cylindrical additive,
ai	initial condition of additive,
af	within melting or freezing region of additive,
ah	within heating region of additive,
am	melting or freezing of additive,
b	frozen bath material or bulk condition of bath material,
bf	within melting or freezing region of bath material,
bm	melting or freezing condition of bath material,
e	interface condition,
max	for maximum frozen layer development,
t	for total time of freezing and melting,

References

- [1] Q.Jiao and N.J.Themelis, 'Mathematical modeling of heat transfer during the melting of solid particles in liquid slag or melt bath.' Canadian Metall. Quarterly, 32 (1), 75-83 (1993).
- [2] E.Rohmen, T.Bergstron, and T.A.Eng, 'Mathematical modeling of heat transfer during the melting of solid particles in liquid slag or melt bath.' INFACON, Trondheim, Norway, 683-695 (1995)
- [3] B.K.Li, X.F.Ma, X.R.Zhang and J.C.He, 'Mathematical model for melting processes of solid particles in metal bath.' Acta Metallurgica Sinica. 12 (3), 259-266 (1999)
- [4] S.Taniguchi, M.Ohmi, and S. Ishiura. 'A hot model study of gas injection upon the melting rate of solid sphere in a liquid bath.' Transactions, ISIJ, 23, 571-577 (1983).
- [5] S.Taniguchi, M.Ohmi, S.Ishiura and S.Yamauchi. 'A cold model study of gas injection upon the melting rate of solid sphere in a liquid bath.' Transactions ISIJ, 23, 565-570 (1983).
- [6] R.Kumar, S.Chandra and A.Chattrjee, 'Kinetics of ferroalloy dissolution in hot metal and steel.' Tata search, 79-85 (1997).
- [7] J.Li, G.Brooks and N.Provatas, Metall. Trans.B, 36 (B), 293-302 (2005).
- [8] L.Pendelaers, F.Verhaeghe, B.Blanpain, P.Wollants and P.Gardin, 'Interfacial reaction during Titanium dissolution in liquid iron. A combined experimental and modeling approach.' Metall. Trans.B, 40 (B), 676-684 (2009).
- [9] L.Pandolaers, F.Verhaeghe, D.Barrier, P.Gardin, P. Wollants and B. Blanpain, 'Theoretical evaluation of influence of convective heat transfer and original sample size on shell melting time during Titanium dissolution in secondary steel melting.' Ironmaking Steelmaking, 37, 516-521(2010).
- [10] S.Sanyal, S.Chandra, S.Kumar and G.G.Roy. 'An improved model of cored wire injection in steel melt.' ISIJ, International, 44, 1157-1165 (2004).
- [11] R.P.Singh and A.Prasad, 'Integral model based freezing and melting of a melt material onto solid additive.' Mathl. Comput. Modeling, 37, 849-862 (2003).
- [12] U.C.Singh, A.Prasad and A.Kumar. 'A lump integral model for freezing and melting of a bath material onto a plate shaped solid additive in agitated bath.' Acta Metallurgica Slovaca, 19 (1), 60-72 (2013).
- [13] U.C.Singh, A.Prasad and A.Kumar, 'Freezing and melting of a bath material onto cylindrical solid additive in an agitated bath.' J. Min. Metall, Sect B- Metall, 2012, Vol.48 (1) B, pp.11-23 (2012).
- [14] U.C.Singh, A.Prasad and A.Kumar. J. Min. Metall. Sec.B-Metall, 49, (3), 245-256 (2013).
- [15] U.C.Singh, 'Ph.D. thesis, Transient Axi-symmetric Conduction Controlled Freezing and Melting of a Surrounding Bath Material Around a cylindrical Shaped Solid Body, Birla Institute of Technology, Mesra, Ranchi, India, (2014).

- [16] B.Zhou, Y.Yang, M.A.Reuter. 'Modelling of Melting behavior of Aluminum Metal in Molten salt and Melt bath.' Extraction of processing division meeting of TMS, Luter, Sweden, 16-20 June, (2002).
- [17] L.Zhang. Steel Research.67 (11), 466-472 (1996).
- [18] L.Zhag and F.Oeters. Steel Research, 70, 128-134 (1999).
- [19] S.A.Arigyropoulos and P.G.Sismansis, 'The Mass Transfer kinetics of Niobium Solution in Liquid Steel.' Metale. Trans. B, 22 (4), 417-428 (1991).
- [20] S.A.Arigyropoulos and P.G.Sismansis. Steel Research, 68(8), 345-354 (1997).
- [21] U.C. Singh, A.Prasad and A.Kumar. Integral model for development of instant interface temperature at time $t=0^+$ of cylindrical solid additive bath system.' Metall. Transactions B, 42B, 800-806 (2011).
- [22] S.Prasad, A.Prasad and A.Kumar. 'Development of instant interface temperature at time $t=0^+$ of low melting temperature cylindrical solid additive-bath system.' Metall. Material Transactions B, 46B (3), 2616-2627 (2015).
- [23] R.P.Singh and A.Prasad. 'Mathematical model for instant interface equilibrium temperature at time $t=0^+$ of solid additive-melt bath system.' Ironmaking and steelmaking, 32, 411-417 (2005).
- [24] M.N. Ozisik, 'Basic Heat Transfer. McGraw Hill KogakushaLtd. Tokyo N.Y (1977)
- [25] F. Kreith and W.Z Black. 'Basic Heat Transfer. Harper and Row, Publisher N.Y. (1980).
- [26] A. Prasad and S.P. Singh. 'Conduction controlled phase change energy storage with radiative heat addition.' Trans. ASME, 166, 218-23. (1994).
- [27] B.T.F. Chung and L.T. Yeh, 'Solidification and melting of material subject to convection and radiation.' (Assumed linear profile), Journal space craft, 12 (6), 329-333 (1975).
- [28] A. Prasad. 'Radiative melting of materials with melt removal.' J. Spacecraft and Rockets, 16, 445-48 (1979)



ISSN 1584 – 2665 (printed version); ISSN 2601 – 2332 (online); ISSN-L 1584 – 2665

copyright © University POLITEHNICA Timisoara, Faculty of Engineering Hunedoara,
5, Revolutiei, 331128, Hunedoara, ROMANIA

<http://annals.fih.upt.ro>